

# Trapped waves of the 27 November 1945 Makran tsunami: observations and numerical modeling

S. Neetu · I. Suresh · R. Shankar · B. Nagarajan · R. Sharma ·  
S. S. C. Shenoi · A. S. Unnikrishnan · D. Sundar

Received: 28 December 2010 / Accepted: 11 May 2011  
© Springer Science+Business Media B.V. 2011

**Abstract** The 27 November 1945 earthquake in the Makran Subduction Zone triggered a destructive tsunami that has left important problems unresolved. According to the available reports, high waves persisted along the Makran coast and at Karachi for several hours after the arrival of the first wave. Long-duration sea-level oscillations were also reported from Port Victoria, Seychelles. On the other hand, only one high wave was reported from Mumbai. Tide-gauge records of the tsunami from Karachi and Mumbai confirm these reports. While the data from Mumbai shows a single high wave, Karachi data shows that

**Electronic supplementary material** The online version of this article (doi:[10.1007/s11069-011-9854-0](https://doi.org/10.1007/s11069-011-9854-0)) contains supplementary material, which is available to authorized users.

S. Neetu (✉) · I. Suresh · A. S. Unnikrishnan · D. Sundar  
National Institute of Oceanography, Dona Paula, Goa 403004, India  
e-mail: neetu@nio.org

I. Suresh  
e-mail: isuresh@nio.org

A. S. Unnikrishnan  
e-mail: as.unnikrishnan@gmail.com

D. Sundar  
e-mail: sundar@nio.org

R. Shankar  
The Institute of Mathematical Sciences, Chennai 600113, India  
e-mail: shankar@imsc.res.in

B. Nagarajan  
Indian Institute of Surveying and Mapping, Survey of India, Hyderabad 500039, India  
e-mail: ngeoid@yahoo.com

R. Sharma  
Geodetic and Research Branch, Survey of India, Dehra Dun 248001, India  
e-mail: rks\_mgw@rediffmail.com

S. S. C. Shenoi  
Indian National Centre for Ocean Information Services, Hyderabad 500055, India  
e-mail: shenoi@incois.gov.in

high waves persisted for more than 7 h, with maximum wave height occurring 2.8 h after the arrival of the first wave. In this paper, we analyze the cause of these persistent high waves using a numerical model. The simulation reproduces the observed features reasonably well, particularly the persistent high waves at Karachi and the single high wave at Mumbai. It further reveals that the persistent high waves along the Makran coast and at Karachi were the result of trapping of the tsunami-wave energy on the continental shelf off the Makran coast and that these coastally-trapped edge waves were trapped in the along-shore direction within a  $\sim 300$ -km stretch of the continental shelf. Sensitivity experiments establish that this along-shore trapping of the tsunami energy is due to variations in the shelf width. In addition, the model simulation indicates that the reported long duration of sea-level oscillations at Port Victoria were mainly due to trapping of the tsunami energy over the large shallow region surrounding the Seychelles archipelago.

**Keywords** Tsunami · Makran subduction zone · Tide-gauge data · Coastally-trapped waves · Tsunami-hazard mitigation

## 1 Introduction

At 21:56 UTC on 27 November 1945, an earthquake ( $M_w$  8.1) occurred in the subduction zone off the Makran coast of Pakistan, with epicentre located on the continental shelf near the coastal town of Pasni (Figs. 1 and 2) (Pendse 1948; Byrne et al. 1992). This earthquake triggered a tsunami that caused widespread damages along the coastal regions of the Arabian Sea. The tsunami and its impact at major locations (Fig. 1) along the Makran coast (Pasni and Ormara), the Pakistan coast (Karachi), the Indian west coast (Mumbai and Karwar), the Oman coast (Muscat), and Seychelles (Port Victoria at Mahe) have been documented in several reports (Ambraseys and Melville 1982; Beer and Stagg 1946; Pendse 1948). An intriguing aspect of these reports is that the leading tsunami wave that arrived at the Makran coast and at Karachi was not high enough to come far inland and inflict damage. However, destructive waves occurred later, several hours after the arrival of the first and these high waves persisted for a long time.

Pendse (1948) reports that the first wave reached Pasni on the Makran coast about half an hour after the earthquake, but greater damage was caused by a wave that came 3.25 h after the first. Ambraseys and Melville (1982) also state that the first wave did not cause much damage. They report that two destructive waves arrived 90–120 min after the first at Pasni and Ormara. Further, they report that high waves persisted for a long duration at Karachi. Pendse (1948) concurs and notes the times of a series of high waves that struck there for a period of  $\sim 3$  h after the arrival of the initial wave. On the other hand, only one high wave was reported (Ambraseys and Melville 1982; Pendse 1948) from Mumbai.

Beer and Stagg (1946) report the sea-level measurements of this tsunami from Port Victoria, Mahe, Seychelles. The first sea-level observation was at 05:47 UTC (7.8 h after the earthquake) when the sea level observed was 30 cm, while the normal level of tide at that time was 4 cm. The sea level rose to 46 cm at 05:52 UTC, dropped down to zero, and then rose again to 37 cm at 06:13 UTC. The travel time of tsunami to Seychelles is  $\sim 6$  h (as computed from our numerical model). In essence, the observations of Beer and Stagg (1946) suggest that sea-level oscillations persisted for more than 2 h at Seychelles.

The prevalent explanation for the destructive waves (along the Makran coast and at Karachi) occurring much later, several hours after the arrival of the first, is the occurrence of secondary tsunamis generated by submarine mudslides triggered by the earthquake

**Fig. 1** The model domain. The color fill is for the bathymetry

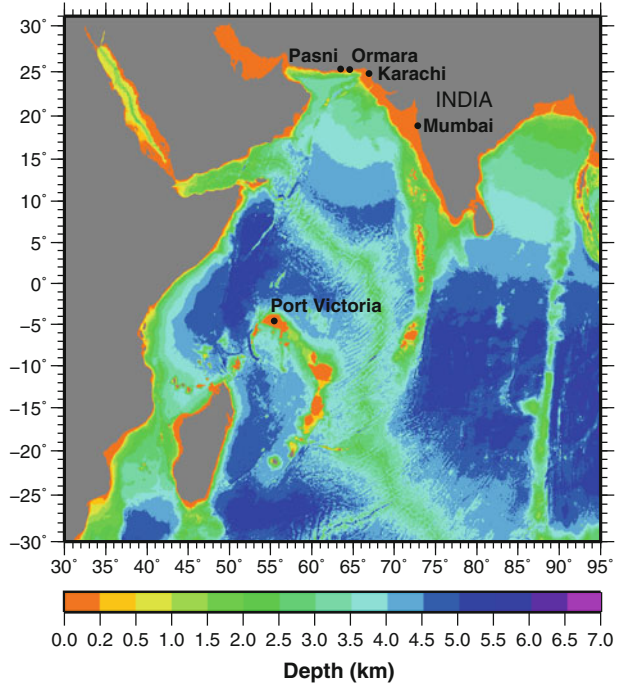
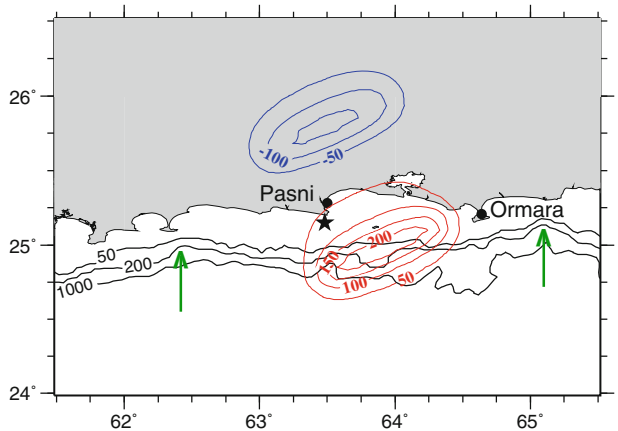


**Fig. 2** Computed vertical deformation (cm) field. Red (Blue) contours represent uplift (subsidence). The asterisk marks the epicentre, and the solid black lines mark the depth (m) contours. The green arrows mark the region of narrowing of the shelf



(Bilham et al. 2007; Rajendran et al. 2008). However, no quantitative analysis of this scenario has been made, i.e., there are no estimates of exactly when and where these mudslides occurred.

The lack of attempts to numerically model such scenarios may be partly due to the lack of continuous sea-level measurements of the tsunami. We present here, for the first time, the sea-level observations of this tsunami from the tide gauges at Karachi (in Pakistan) and Mumbai (then called Bombay, in India). The data, discovered in the archives of the Survey of India, allow us to validate a numerical model of the tsunami propagation. Using numerical model simulation of the event with earthquake as the only source of tsunami, we show that the persistent high waves were the result of trapped modes excited by the

tsunami, and there is no need to invoke mudslides to explain the reported phenomena and the observations.

## 2 The data

The tide gauges at Karachi and Mumbai were maintained by the Survey of India (SOI) during this tsunami event. The analog records from SOI archives were digitized at a sampling interval of 1 min. The observed sea levels (Fig. 3) were subjected to a high-pass, eighth-order Butterworth filter (Emery and Thomson 1998) with a cut-off period of 3 h to remove the tide. The high-passed, de-tided data (Fig. 4), that is the residual, retain only the sea-level perturbations due to tsunami.

The time of arrival of the first tsunami wave at Karachi was 23:30 UTC, with a wave height of 28 cm (Fig. 4). The maximum wave height (44 cm) occurred at 02:19 UTC, 2.8 h after the arrival of the first wave. Consistent with the reports (Ambraseys and Melville 1982; Pendse 1948), the data shows that waves of high amplitude persisted for more than 7 h after the arrival of the first wave. The timings of wave peaks seen in the residual data match those reported by Pendse (1948). At Mumbai, the tsunami arrived at 02:37 UTC (Fig. 4). The first wave was the highest with an amplitude of 34 cm. The amplitudes of subsequent waves were less than one-third of the first wave. This is also consistent with Pendse (1948).

## 3 Numerical modeling

A detailed analysis of this earthquake has been published by Byrne et al. (1992). They concluded that it was an interplate thrust event that ruptured about one-fifth length of the Makran Subduction Zone. The north-south extent of the rupture zone was about 100 km,

**Fig. 3** The observed sea levels, which include the tide, at Karachi and Mumbai. The tide gauge at Karachi had malfunctioned before the tsunami struck there. The officer in charge of the tide gauge had marked on the chart that the gauge was out of order. Fortunately, the gauge had resumed recording just before the arrival of the initial wave. Also there is another gap in the data between 4.83 and 5.05 h after the earthquake

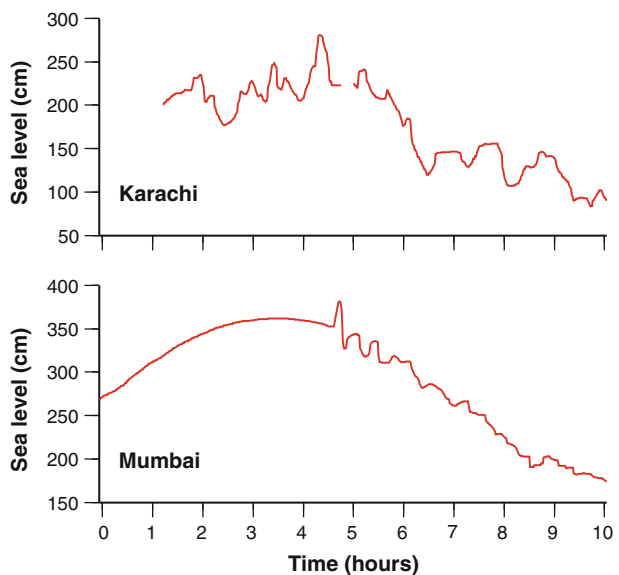
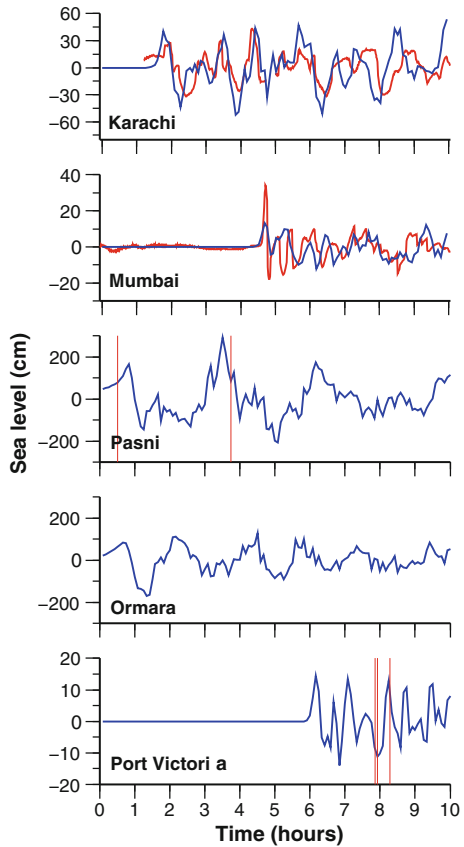


**Fig. 4** The blue (red) lines mark the modeled (observed) sea levels. The comparison between model and data is shown for Karachi and Mumbai. The horizontal axis starts at the origin time of earthquake. The observational timings at Pasni reported by Pendse (1948) and at Port Victoria reported by Beer and Stagg (1946) are marked with the red vertical lines



with  $\sim 30$  km extending seaward from the coast. We used the earthquake source parameters (Table 1) estimated by them to compute the static vertical displacement field of the sea floor and the land from Okada’s solution (Okada 1985) (Fig. 2). The fault model implies that the sea-floor deformation was almost entirely confined to the  $\sim 100$ -km wide shelf-slope region. The initial sea-level distribution was assumed to be the same as that of the sea-floor deformation (Fig. 2) and was used as an initial condition for a numerical model of tsunami propagation.

**Table 1** The earthquake source parameters estimated by Byrne et al. (1992)

Length of the fault plane	100 km
Width of the fault plane	100 km
Epicentre of the earthquake	63.48°E, 25.15°N
Focal depth	15 km
Strike	246°
Dip	7°
Rake	89°
Slip	7 m

The tsunami propagation was modeled using non-linear shallow-water equations on the sphere with Coriolis force and bottom friction included. The governing (momentum and continuity) equations on the sphere are

$$\frac{\partial U}{\partial t} = -\frac{1}{R \cos y} \frac{\partial(uU)}{\partial x} - \frac{1}{R} \frac{\partial(vU)}{\partial y} - \frac{g(h + \eta)}{R \cos y} \frac{\partial \eta}{\partial x} + fV - C_D \frac{U\sqrt{U^2 + V^2}}{(h + \eta)^2},$$

$$\frac{\partial V}{\partial t} = -\frac{1}{R \cos y} \frac{\partial(uV)}{\partial x} - \frac{1}{R} \frac{\partial(vV)}{\partial y} - \frac{g(h + \eta)}{R} \frac{\partial \eta}{\partial y} - fU - C_D \frac{V\sqrt{U^2 + V^2}}{(h + \eta)^2},$$

and

$$\frac{\partial \eta}{\partial t} = -\frac{1}{R \cos y} \frac{\partial U}{\partial x} - \frac{1}{R} \frac{\partial V}{\partial y} + \frac{\tan y}{R} V,$$

where  $x$  is the longitude and  $y$  is the latitude.  $U = u(h + \eta)$  and  $V = v(h + \eta)$  are the horizontal transports,  $u$  and  $v$  being the depth-averaged horizontal velocities;  $h$  and  $\eta$  denote the undisturbed depth of the water column and the sea-surface elevation, respectively, and  $t$ ,  $g$ ,  $R$ ,  $C_D$ , and  $f$  are, respectively, the time, the acceleration due to gravity, the radius of the earth, the bottom drag coefficient (the value of which is set to 0.001), and the Coriolis parameter given by  $f = 2\Omega \sin y$ , where  $\Omega$  is the angular velocity of the earth.

The energy density,  $E(J/m^2)$ , at a model grid point was calculated as

$$E = \rho \left\{ \frac{(h + \eta)}{2} (u^2 + v^2) + \frac{g}{2} \eta^2 \right\},$$

where  $\rho$  is the constant water density (set to 1,000 kg/m<sup>3</sup>).

The finite-difference computations were made on an Arakawa-C grid using the leap-frog scheme. The model domain (Fig. 1) covered the region of the Indian Ocean from 30°E to 95°E and from 30°S to 31°N, encompassing the regions of our interest in this study (Makran coast, Karachi, Mumbai, and Seychelles). We used the no-slip condition at continental boundaries and an open-boundary (radiation) condition at the open-ocean boundaries at the southern and eastern ends of the domain. The spatial grid size was 1 arc min and the time step was 2 s to satisfy the CFL (Courant-Friedrichs-Levy) stability condition. We used the improved 2-arc min bathymetry for the Indian Ocean generated by Sindhu et al. (2007); the bathymetry on the 1-min grid was obtained using bilinear interpolation.

The modeled sea levels compare reasonably well with the observed residuals at Karachi (including the persistent high waves) and at Mumbai (Fig. 4) in terms of amplitude, period, and phase of individual waves. Since our model does not include any secondary sources like submarine mudslides, we conclude that this tsunami was primarily caused by the earthquake.

## 4 Discussion

### 4.1 The mechanism of persistent high waves

Since the model captures the patterns of variability in the tide-gauge observations (Fig. 4), we used it to understand the cause of the persistent high waves reported from the Makran coast, Karachi, and Seychelles by examining the model dynamics in detail and by performing some numerical experiments.

4.1.1 The Makran coast

The model simulation shows that the tsunami generated on the shelf-slope region by the earthquake propagated both offshore and onshore (Fig. 5a and Movies 1, 2 in the online resource). A significant fraction of the offshore-propagating energy was reflected back to the shelf from the shelf break, the rest was transmitted to the open sea and created the first wave observed at Karachi and Mumbai (Fig. 4). This partial reflection at the shelf break is due to rapid changes in the depth along the cross-shore direction, leading to rapid changes in the wave speed. The physics is analogous to the partial reflections seen from a transparent glass sheet.

Much of the tsunami-wave energy was therefore trapped on the shelf. The trapped energy would normally have propagated away in the along-shore direction as coastally trapped edge waves (LeBlond and Mysak 1978; Mysak 1980). The shelf off the Makran coast narrows at around 62°E and 65°E (Fig. 2) implying a rapid change in depth in the along-shore direction as well. This leads to partial reflections of edge waves at around 62°E and 65°E, thus localizing the wave energy for many hours (Fig. 5b) on the shelf between these two longitudes where the shelf gets pinched.

This mechanism of wave localization was confirmed by performing numerical experiments. In the first experiment (EXP1), we created an idealized bathymetry by setting the inclinations of the continental shelf and the slope to the average inclinations of the continental shelf and the slope off the Makran coast, respectively (Fig. 6). The shelf width was uniform in this idealized bathymetry. Consistent with the theory (LeBlond and Mysak 1978;

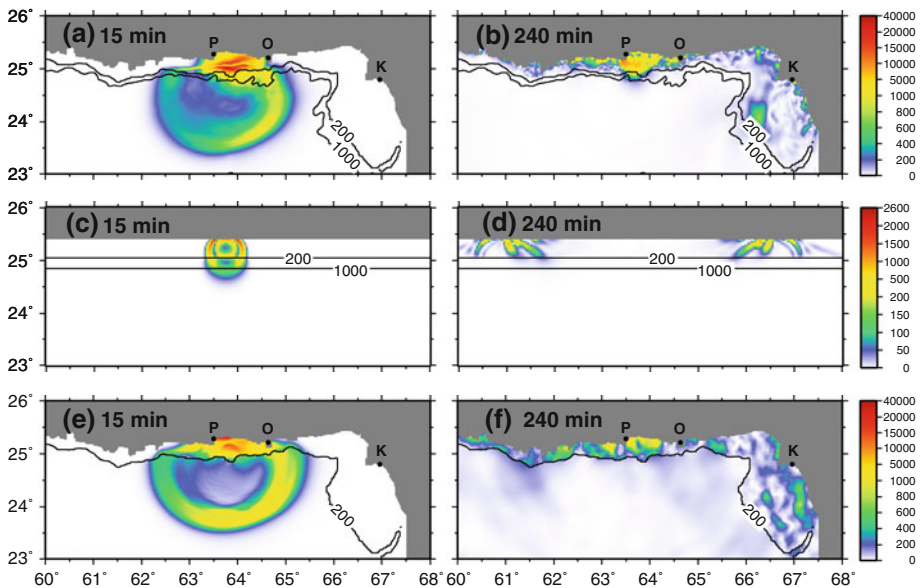


**Fig. 5** Snapshots of the computed energy density ( $J/m^2$ ). The solid black lines represent the depth (m) contours. The black dots mark the locations of Pasi (P), Ormara (O), and Karachi (K). The time marked on the top-left corner is the time lapsed after the earthquake. Figures (a) and (b) are from the main simulation, (c) and (d) are from EXP1, (e) and (f) are from EXP2. The energy levels of the main simulation, EXP1, and EXP2 are not directly comparable to each other due to differences in the bathymetry and initial conditions between the runs. For EXP1, we used a Gaussian tsunami source of width  $\sim 50$  km on the shelf. The initial condition for EXP2 is same as that of the main run

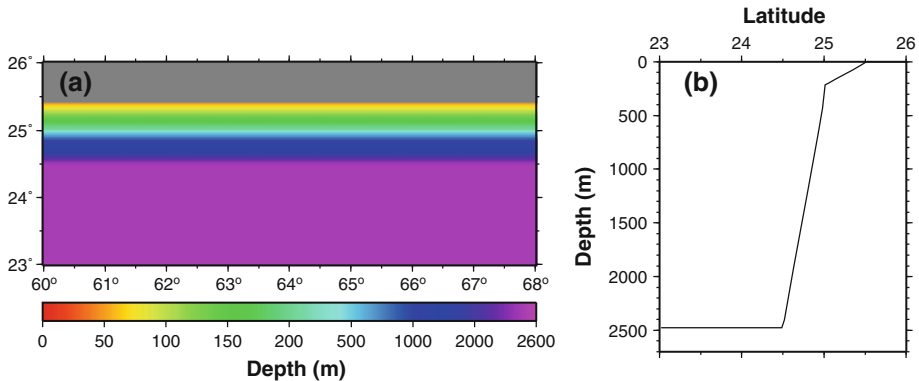


**Fig. 6** (a) The idealized bathymetry of the experiment EXP1. (b) Depth profile across the coast in EXP1

Mysak 1980), the coastally-trapped edge waves propagated parallel to the coast and were not localized in the along-shore direction in this experiment (Fig. 5c, d). In another experiment (EXP2), the shelf geometry was retained and the irregularities in the bathymetry were removed by setting the depths less than 200 m to 200 m and depths greater than 200 m to 2,000 m (Fig. 7). Specifically, this idealized bathymetry mimics the narrowing feature of the shelf off the coast of Makran. In this experiment, the coastally-trapped modes on the shelf were localized in the along-shore direction (Fig. 5e, f) as in the case of main simulation (Fig. 5a, b), indicating that the wave localization was due to the narrowing of the shelf.

Thus the shelf topography gave rise to localized modes that were trapped both in cross-shore and along-shore directions in a region between  $\sim 62^\circ\text{E}$  and  $\sim 65^\circ\text{E}$  (Fig. 5a, b). Model results show that for nearly 4 h following the earthquake, the energy trapped in this  $\sim 300\text{-km}$  shelf regime was more than half the total energy of the tsunami (Fig. 8).

The details of dynamics in the Pasni-Ormara region can be understood from the model simulation (Movie 2 in the online resource). Initially, the wave energy peaked at the earthquake epicentre. Most of it propagated in the off-shore direction, but a large fraction is reflected at the shelf break. This high energy packet hit the coast about 80 min after the earthquake almost halfway between Pasni and Ormara. It was reflected from the coast, propagated to the shelf break and again much of the energy is reflected back from there (about 2.5 h after the earthquake). It then propagated back to the coast and hit Pasni about 3.5 h after the earthquake (3.75 h according to Pendse 1948). The modeled sea levels (Fig. 4) at Pasni and Ormara show that high waves persisted for several hours.

#### 4.1.2 Karachi and Mumbai

The first offshore pulse propagated over the deep sea and was the first wave to arrive at Karachi and Mumbai (Fig. 5a and Movie 1). Some of the energy of the first offshore pulse and the energy leaking from the region of narrowing of the shelf near  $65^\circ\text{E}$  made it east of  $65^\circ\text{E}$  (Movie 2) and propagated eastward and southward along the shelf as packets of edge waves guided by local topography. Their arrivals at Karachi led to persistent high waves there (Fig. 4). Their amplitude, simulated rather well by our model, was determined by the details of topography. These edge waves did not propagate all the way to Mumbai, presumably due to frictional damping and abrupt changes in the coastline. Thus there was only one high wave at Mumbai.

**Fig. 7** Idealized bathymetry of the experiment EXP2

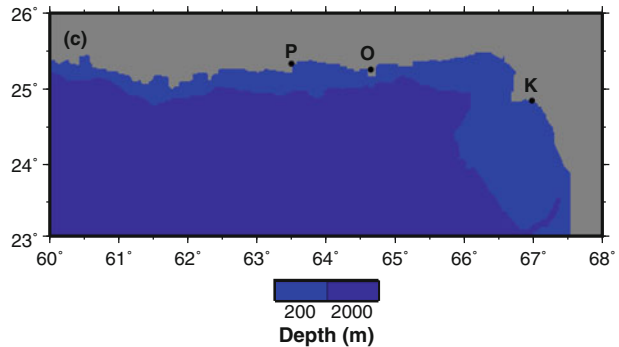
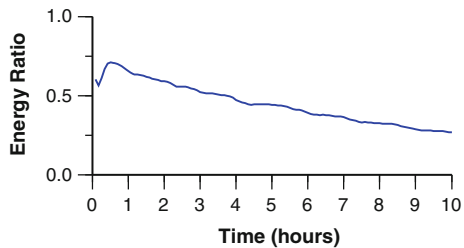


**Fig. 8** Ratio of the energy trapped on the shelf (between 0 and 200 m depths) between 62°E and 65°E to the total energy in the model domain. The horizontal axis starts at the origin time of earthquake



### 4.1.3 Seychelles

The modeled sea level at Port Victoria, Seychelles, shows that the oscillations due to tsunami persisted for several hours (Fig. 4). Seychelles archipelago is surrounded by a large, shallow shelf (Fig. 1). The simulation (Movie 3) shows that when the leading wave arrived in the shallow region, it got amplified as expected (Fig. 9a) and remained trapped there owing to waves reflecting back from the shelf break (Movie 3). The trapped energy bounced around on the shelf for several hours (Fig. 9b, Movie 3). The trapped waves were also scattered (Movie 3) by the islands within the shelf leading to a complex wave pattern.

## 5 Conclusions

Available reports (Ambraseys and Melville 1982; Beer and Stagg 1946; Pendse 1948) of the historic 1945 Makran tsunami indicate that high waves persisted for several hours after the arrival of the initial wave along the Makran coast, at Karachi, and at Seychelles, but there was only one high wave at Mumbai. The data from Karachi and Mumbai tide gauges are consistent with these reports. We have modeled the event numerically, with earthquake as the only source of tsunami. Based on the simulation and the sensitivity experiments, we show that the persistent high waves were due to excitation of trapped modes by the tsunami on the continental shelf.

While there is evidence that the earthquake might have triggered submarine mudslides (Ambraseys and Melville 1982; Byrne et al. 1992), our results show that it is not necessary to invoke any secondary source like mudslides to explain the tide-gauge data and the reports mentioned above.

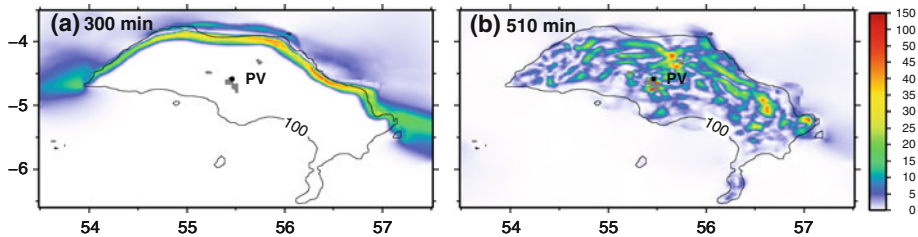


**Fig. 9** Snapshots of the computed energy density ( $J/m^2$ ) from the main simulation. The solid black line represent the 100-m depth contour. The black dot marks the location of Port Victoria (PV). The time marked on the top-left corner is the time lapsed after the earthquake

Our study also has important implications for tsunami-hazard assessment and mitigation. Though the hazard posed by trapped edge-wave modes excited by tsunamis generated on shelves has been known earlier (see e.g. Gonzalez et al. 1995), the additional potential threat revealed by our study is that these modes could further be trapped in the along-shore direction due to longshore variations in the shelf width. Hence, for tsunamis generated on a shelf, destruction depends on the details of shelf topography, which can trap the energy, leading to greater-than-expected, but localized damage. Study of topographic details on tsunamigenic shelves would make tsunami-hazard preparedness more effective.

**Acknowledgments** We thank Yuichiro Tanioka for providing software for computing Okada's solution and the Surveyor General of India for the tide-gauge data. We thank S. R. Shetye and D. Shankar for useful discussions. We thank Matthieu Lengaigne for his valuable comments on the manuscript. We acknowledge Indian National Centre for Ocean Information Services, Hyderabad, and Council of Scientific and Industrial Research, New Delhi, for financial support. This is NIO contribution 4976.

## References

- Ambraseys NN, Melville CP (1982) A history of persian earthquakes. Cambridge University Press, New York, pp 89–90
- Beer A, Stagg JM (1946) Seismic sea-wave of November 27, 1945. *Nature* 158(4002):63
- Bilham R, Lodi S, Hough S, Bukhary S, Khan AM, Rafeeqi SFA (2007) Seismic hazard in Karachi, Pakistan: uncertain past, uncertain future. *Seis Res Lett* 78:601–613
- Byrne DE, Sykes LR, Davis DM (1992) Great thrust earthquakes and aseismic slip along the plate boundary of the Makran subduction zone. *J Geophys Res* 97(B1):449–478
- Emery WJ, Thomson RE (1998) Data analysis methods in physical oceanography. Pergamon, Oxford, pp 540–549
- Gonzalez FI, Satake K, Boss EF, Mofjeld HO (1995) Edge wave and non-trapped modes of the 25 April 1992 Cape Mendocino tsunami. *PAGEOPH* 144:409–426
- LeBlond PH, Mysak LA (1978) Waves in the ocean. Elsevier Scientific Publishing Company, Amsterdam, pp 219–227
- Mysak LA (1980) Topographically trapped waves. *Ann Rev Fluid Mech* 12:45–76
- Okada Y (1985) Surface deformation due to shear and tensile faults in a half-space. *Seismol Soc Am* 75:1135–1154
- Pendse CG (1948) The Mekran earthquake of the 28th November 1945. *Sci Notes Indian Meteorol Dep* 10:141–144
- Rajendran CP, Ramanamurthy MV, Reddy NT, Rajendran K (2008) Hazard implications of the late arrival of the 1945 Makran tsunami. *Curr Sci* 95:1739–1743
- Sindhu B, Suresh I, Unnikrishnan AS, Bhatkar NV, Neetu S, Michael GS (2007) Improved bathymetric datasets for the shallow water regions in the Indian Ocean. *J Earth Syst Sci* 116:261–274